https://doi.org/10.37434/tpwj2021.03.01

FATIGUE LIFE OF STEEL 40Kh SPECIMENS AFTER WEAR-RESISTANT SURFACING WITH A SUBLAYER OF LOW-CARBON STEEL

I.O. Ryabtsev, V.V. Knysh, A.A. Babinets and **S.O. Solovej**
E.O. Paton Electric Welding Institute of the NAS of Ukraine
11 Kazymyr Malevych Str., 03150, Kyiv, Ukraine. E-mail: office@paton.kiev.ua

The resistance to fatigue fracture of steel 40Kh after wear-resistant surfacing using PP-Np-25Kh5FMS flux-cored wire with a sublayer of a low-carbon ductile material formed by Sv-08A wire was investigated. The design of the deposited specimens and the procedure of their testing simulated operating conditions of the mill rolls, for surfacing of which PP-Np-25Kh5FMS flux-cored wire is widely used. A comprehensive procedure for evaluating the resistance of multilayer material to fatigue fracture included three stages: determination of cyclic life of specimens after manufacturing surfacing; study of cyclic crack resistance of different metal layers; determination of fatigue life of specimens, which in the course of preliminary tests had fatigue cracks in the deposited layer after repair surfacing. It was established that the cyclic life of the specimens of carbon steel 40Kh, deposited using PP-Np-25Kh5FMS flux-cored wire with a sublayer of low-carbon steel 08kp (rimmed) exceeds the cyclic life of the specimens deposited without a sublayer, approximately by 2 times. The maximum values of stress intensity factor (SIF) (140–180 MPa√m) obtained on the specimens with a multilayer surfacing with a sublayer, are 2–3 times higher than the maximum values of SIF obtained on the specimens without a sublayer, which indicates the rationality of using a low-carbon sublayer to increase the crack resistance of a multilayer material with wear-resistant surfacing. It was shown that performance of repair surfacing according to the scheme of removal and a subsequent remelting of only areas of the metal with fatigue cracks of long-term operating parts does not lead to a significant increase in the cyclic life after repair. This is related to the fact that after long operation, the defect-free layer of deposited metal has a significant level of accumulated fatigue damages. Therefore, to increase the efficiency of repair surfacing, it is recommended to remove not only the metal around the detected fatigue cracks, but the entire deposited layer to the depth of detected fatigue cracks with the subsequent restoration surfacing. 18 Ref., 4 Tables, 7 Figures.

K e y w o r d s : arc surfacing, repair surfacing, ductile sublayer, fatigue life, fatigue cracks, stress intensity factor

Most parts and units of industrial equipment of metallurgical and machine-building industries are operated under the conditions of variable cyclic load [1]. One of such parts is rolls of rolling mills which, depending on operating modes, fail as a result of fatigue, surface wear or combination of the mentioned factors. For example, the rolls of breakdown mills are exposed to thermal fatigue, which leads to the appearance of a grid of small cracks on the surface of rolls, which can further propagate as fatigue cracks. It is difficult to predict the moment of origination and the rate of propagation of defects of such type, so it can lead to the fracture of a roll [1–6]. Annually, on replacement of worn parts and elements of equipment up to 5–30 % from the total cost of manufactured products is spent [5]. This indice can be reduced by extending the life of damaged large-size parts due to repair and restoration works with the use of surfacing the metal layer with improved service properties relative to the base metal.

The technology of manufacturing or repair surfacing can be performed both without surfacing of the intermediate metal layer (sublayer) as well as with it. Thus, in [7], the data on the technology of surfacing specimens of carbon steel 40Kh, simulating the design of a rolling mill, with the use of flux-cored wire PP-Np-25Kh5FMS without a sublayer are given. The authors experimentally established the cyclic life and characteristics of crack resistance of the metal of the deposited specimens. However, it is known that to improve weldability of the base and wear-resistant metal, as well as to reduce residual stresses, it is rational to perform a preliminary surfacing of a sublayer on the base metal with an intermediate value of the thermal expansion coefficient. For this purpose, often surfacing of the intermediate layer of low-carbon and low-alloy materials of type Sv-08A, Sv-08G2S, etc. is used. [8]. To determine the most effective surfacing technology (with or without a sublayer) it is necessary to conduct a comparative evaluation of fatigue life of

I.O. Ryabtsev — https://orcid.org/0000-0001-7180-7782, V.V. Knysh — https://orcid.org/0000-0003-1289-4462,
A.A. Babinets — https://orcid.org/0000-0003-4432-8879, S.O. Solovej — https://orcid.org/0000-0002-1126-5536

© I.O. Ryabtsev, V.V. Knysh, A.A. Babinets and S.O. Solovej, 2021

multilayer deposited parts and specimens with and without a sublayer.

The calculated determination of fatigue life of multilayer deposited parts is quite complicated. This is explained by several factors. First, surfacing of several layers of the metal different as to chemical composition leads to a complex stress state in multilayer specimens. For example, as a result of redistribution of stresses during surfacing of subsequent layers of metal, the initially obtained residual compressive stresses can be converted into tensile stresses, which negatively affect the fatigue life [2, 9]. Secondly, with an increase in the number of deposited beads and/or layers on the base metal, the probability of formation of such single defects as pores, inclusions, slags, etc., which significantly reduce the fatigue life, increases [10–12]. Therefore, to establish the rationality of using a metal sublayer during surfacing in order to increase the life of multilayer deposited specimens, it is more rational to use experimental procedures for evaluation of fatigue life.

Thus, the aim of this work is an experimental study of the influence of materials and technologies of manufacturing and repair surfacing of wear-resistant working layer and sublayer on the fatigue life of multilayer deposited parts.

Procedures, technologies and investigation materials. To establish the rationality of using a metal sublayer during surfacing in order to increase the fatigue life of multilayer deposited specimens, the technology of surfacing specimens without a sublayer was used, which is described in detail in [7, 13]. The main stages of technology of producing deposited specimens are: preheating of billets of steel 40Kh to 250–300 °C; at first, automatic arc surfacing of a sublayer material with a total thickness of 4–5 mm and a wear-resistant layer with a thickness of ≈ 6 mm; slowered cooling of deposited specimens together with the furnace.

The steel grades of the base metal and the deposited wear-resistant metal layer (steel 40Kh and 25Kh-5FMS, respectively) were identical during surfacing of the specimens without a sublayer and with a sublayer. For surfacing of the intermediate layer, a solid low-carbon wire Sv-08A was used, and for surfacing of the wear-resistant layer, flux-cored wire PP-Np-25Kh5FMS with the diameters of 1.8 mm was used. The surfacing mode for all the specimens was the same: I = 220–250 A; U = 26–28 V; V = 18 m/year; beads overlapping ≈ 50 %. According to the above-mentioned technology, 3 series of prismatic specimens with dimensions of 350×40×20 mm with the quantity of 3–5 specimens in each series were made. The chemical composition and mechanical properties of the materials used in the work are given in Tables 1 and 2 [14].

The first series of specimens was tested for fatigue until their complete fracture or until reaching the test base of $2 \cdot 10^6$ cycles of stress changes. Fatigue tests were performed in a test servohydraulic machine URS-20 at a three-point bending with a cycle asymmetry of R_σ = 0 and a frequency of 5 Hz under the

Table 1. Chemical composition of base and deposited metals [14]

Grade of material	Mass fraction of elements, %							
	C	Mn	Si	Cr	V	Mo	S	P
40Kh	0.36–0.40	0.5–0.8	0.17–0.37	0.8–1.1	–	–	≤0.035	≤0.035
Sv-08A*	0.05–0.12	0.2–0.4	≤0.03	≤0.10	–	–	≤0.04	≤0.04
PP-Np-25Kh5FMS*	0.20–0.32	0.5–1.0	0.80–1.30	4.6–5.8	0.2–0.6	0.9–1.5	≤0.04	≤0.04
4Kh5MFS**	0.32–0.40	0.2–0.5	0.90–1.20	4.5–5.5	0.3–0.5	1.2–1.5	≤0.04	≤0.04

*Mass fraction of elements in the deposited metal is given.
**Data on mechanical properties of the metal deposited with the wires Sv-08A and PP-Np-25Kh5FMS are absent in the literature. Therefore, data for their analogues are given (the closest as to the chemical composition and mechanical properties), respectively to steels 08kp and 4Kh5MFS.

Table 2. Mechanical properties of base and deposited metals [14]

Grade of material	Mechanical properties (after normalization)					
	Conditional yield strength $\sigma_{0.2}$, MPa	Ultimate tensile strength σ_t, MPa	Relative elongation δ, %	Relative reduction in area ψ, %	Impact toughness *KCU*, J/cm^2	Hardness *HV*
40Kh	345	590	12.5	52	7.5	174–217
08 kp**	196	320	33	60	–	≤131
Sv-08A*	1570	1710	12	54	51	444–478

*Data on mechanical properties of the metal deposited with the wires Sv-08A and PP-Np-25Kh5FMS are absent in the literature. Therefore, data for their analogues are given (the closest as to the chemical composition and mechanical properties), respectively to steels 08kp and 4Kh5MFS.

conditions of regular loading. The distance between the supports was 250 mm.

At the second series of specimens cyclic crack resistance was evaluated. To initiate the propagation of a fatigue crack in the deposited metal in the center of the specimen (in the area of maximum applied stresses), a V-shaped notch of 1.0–1.5 mm depth with 0.25 mm radius was made. After that, at a three-point cyclic bending with a maximum level of applied stresses in the cross-section of the specimen being 400 MPa, a fatigue crack was grown until reaching a length of 1 mm on a one of the side faces. The resulted notch with a crack was taken as an initial fatigue crack in the test specimen, which was then used to study the kinetics of fatigue fracture. While performing the fatigue tests on cyclic crack resistance, the length of the propagated fatigue crack was measured using an optical microscope with a division value of 0.01 mm on the two side faces of the specimen and then averaged. The tests were performed until a complete fracture of the specimens.

On the specimens of the third series, the efficiency of applying repair surfacing to increase the residual cyclic life of the specimens, having fatigue cracks in the deposited wear-resistant layer was investigated. The specimens were tested for fatigue at a three-point bending with a cycle asymmetry $R_\sigma = 0$ to the formation of a fatigue crack with a depth of 10–12 mm (when a crack passed through the deposited layers and deepened into the base metal). After that, repairs were carried out applying the method of arc surfacing, which consists of a complete mechanical removal of a fatigue crack and the metal around it and a subsequent remelting of the formed groove. The technology of repair surfacing is described in more detail in [7].

To study the nature of fatigue crack propagation in the deposited specimens after their repair, a metallographic microscope MIM-7 was used, equipped with a video eyepiece SIGETA MCMOS 3100. This video eyepiece is supplied with the software Toupview, used to perform digital processing of the obtained photographs and calculation of crack sizes at magnifications of ×0–×320. Before the measurements, the microscope was calibrated using a micrometer object.

In addition, before the fatigue test in the specimens after repair surfacing, residual stresses were measured applying a non-destructive acoustic method using a portable ultrasonic stress control device [15].

Table 3. Results of fatigue tests of specimens of the first series

Number of specimen	Maximum cycle stresses, MPa	Cyclic life before fracture, cycles
1	500	>2000000
2	500	>2000000
3	600	>2000000
4	600	775100*
5	600	>2000000

*Defect in the fusion zone between the sublayer and wear-resistant layer.

Results of experiments and their discussion. Initially, two specimens of the first series of carbon steel 40Kh, deposited using flux-cored wire PP-Np-25Kh5FMS with a sublayer of low-carbon steel 08kp, were tested at maximum stress levels of 500 MPa, typical for the specimens made without a sublayer [11]. After operation of specimens during $2 \cdot 10^6$ cycles, no changes in fatigue crack stresses were detected. It should be noted that fracture of the specimens without a sublayer at maximum stress levels of 500 MPa occurred in the range from 560800 to 1420100 cycles of stress changes [11]. The other three specimens, deposited with a sublayer, were tested at the levels of maximum stresses increased to 600 MPa. The results of fatigue tests of the first series of specimens are given in Table 3.

An early fracture of the specimen No.4 of the first series after 775100 cycles was predetermined by the presence of a surfacing defect in the transition zone of a sublayer metal to the metal of a wear-resistant layer. Thus, the defect-free specimens with a sublayer of low-carbon steel withstood more than $2 \cdot 10^6$ cycles of stress changes at maximum stresses of 500–600 MPa. Therefore, the use of a sublayer of low-carbon steel in surfacing of a wear-resistant layer allowed increasing the life of the specimens after manufacturing surfacing by almost 2 times as compared to surfacing of the specimens without a ductile sublayer.

On three specimens of the second series from the sharp notch in a wear-resistant layer of metal, an initial crack with a depth of 1 mm was grown at maximum stress levels of 400 MPa. In the subsequent tests of the specimen also at the levels of maximum stresses of 400 MPa, the length of a fatigue crack and the corresponding number of cycles of a variable load N were recorded.

It was established that the main crack mainly propagates predominantly along the fusion boundary of individual beads. In the process of fatigue fracture, as a result of variable loads of a one metal layer to another in the transition zones, slight side branching from the main crack were observed, which propagated along the fusion line of a wear-resistant metal layer with a sublayer metal (Figure 1) and along the fusion line of a sublayer metal with the base metal (Figure 2). After the crack passed through a wear-resistant layer of metal and a sublayer of a low-carbon steel, the fracture of the specimens occurred on the base metal.

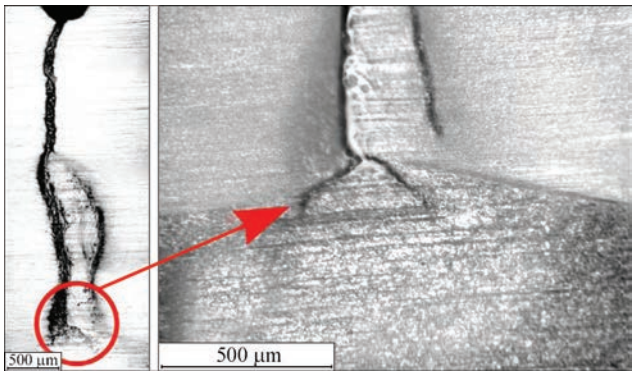

Figure 1. Branching of fatigue crack in the fusion zone of wear-resistant layer and ductile sublayer

This can be explained by several factors. First, in the area of overlapping adjacent deposited beads, the zone of chemical and structural heterogeneity is located, which negatively affects the properties of the material [1]. Secondly, during multibead multilayer surfacing, at the fusion boundary of adjacent beads and layers sharp angles may occur, which will be stress concentrators and, accordingly, initiate the formation of side cracks along the fusion line [16, 17]. After the crack passes through the wear-resistant layer of metal and the sublayer of low-carbon steel, the fracture of the specimens occurred on the base metal. Thus, the same as for the specimens deposited without a sublayer, it was found that the fusion lines of individual beads and layers play an important role in the process of fatigue fracture of deposited parts, as cracks mainly propagate either along the fusion of individual beads, or directly near this boundary (Figure 2). The only difference between these two surfacing technologies in relation to fatigue crack propagation is the formation of small side branching from the main crack (Figures 1, 2).

To construct kinetic diagrams of fatigue fracture (KDFF), the values of the stress intensity factor (SIF) were calculated from the expressions for a three-point load of a prismatic specimen with a cross edge crack [18]. The experimental dependence of fatigue crack growth rate on the SIF range in different layers of

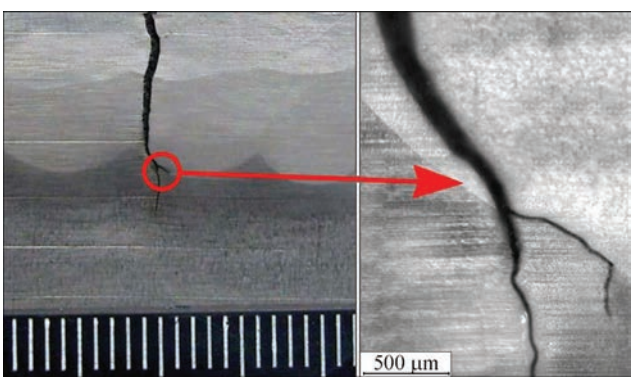

Figure 2. Branching of fatigue crack in the fusion zone of sublayer with base metal

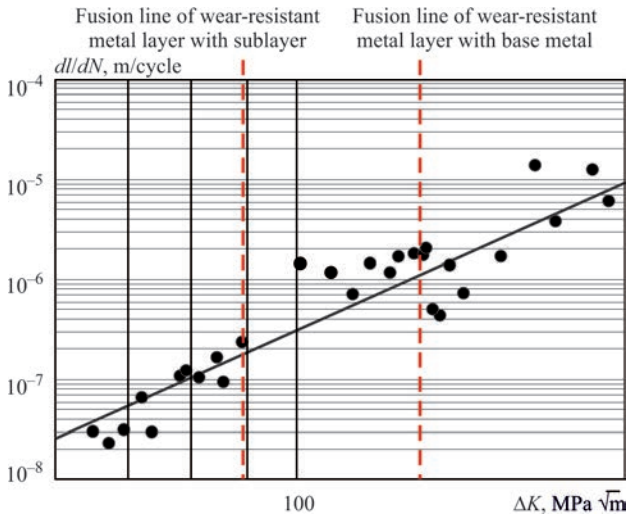

Figure 3. Kinetic diagram of fatigue fracture of multilayer material, formed by wear-resistant surfacing with the use of sublayer of low-carbon steel

metal in a multilayer specimen is given in the form of KDFF (Figure 3). The obtained data show that at the set levels of maximum stresses of 400 MPa, the range of changes in the growth rate of fatigue cracks in the multilayer material corresponds to the linear area of KDFF, and, accordingly, it can be described by the degree dependence of Paris $dl/dN = C(\Delta K)^m$ with the parameters $C = 5.75 \cdot 10^{-17}$ and $m = 4.87$. The maximum SIF values (140–180 MPa√m) on the specimens with a multilayer surfacing with a sublayer, 2–3 times exceed the maximum SIF values obtained on the specimens without a sublayer [7], which indicates the rationality of using a low-carbon sublayer to increase the crack resistance of a multilayer material with a wear-resistant surfacing.

On the specimens of the third series, at first initiation and propagation of fatigue cracks from probable defects in the deposited wear-resistant metal layer were modeled. Therefore, the specimens were tested under a cyclic loading until the formation of fatigue cracks with a depth of 10–12 mm, which were subsequently removed by repair surfacing. After repair surfacing, residual stresses were measured applying a non-destructive ultrasonic method. Schematic representation of places of residual stress measurement is

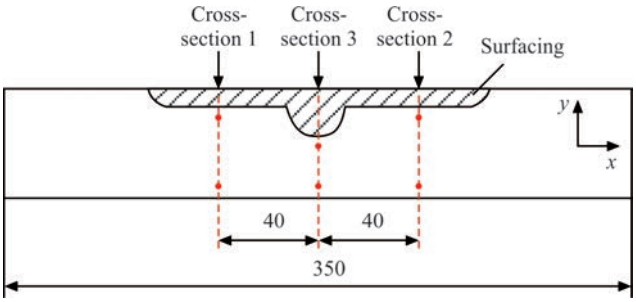

Figure 4. Schematic image of places of measuring residual stresses in the specimen after repair surfacing

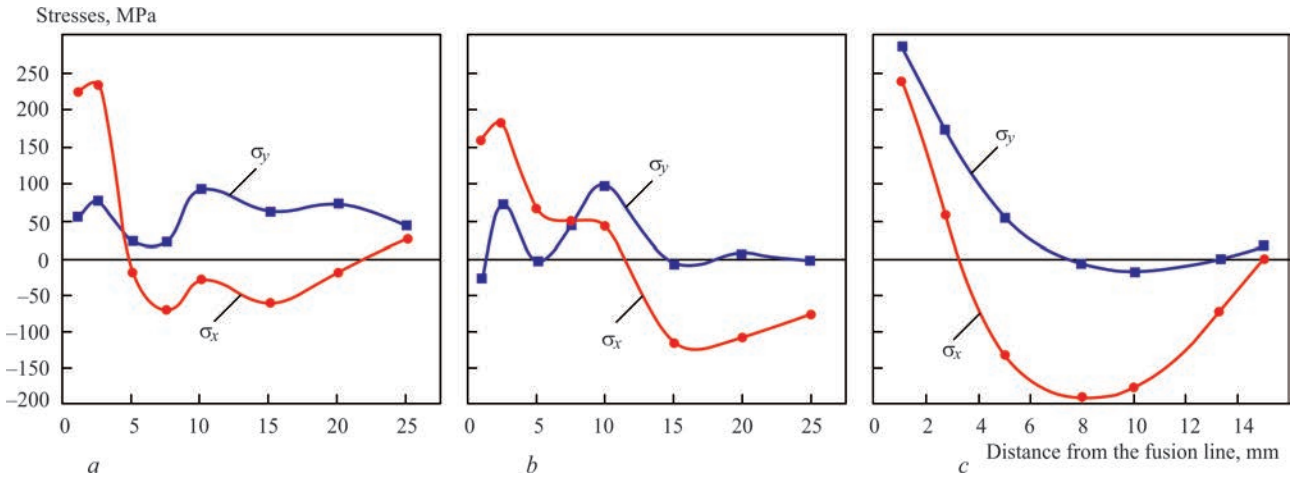

Figure 5. Distribution of residual stresses oriented along σ_x and across σ_y of the specimen after repair surfacing in the cross-section 1 (*a*), 2 (*b*) and 3 (*c*)

shown in Figure 4, and plots of distribution of residual stresses in the initial state and after repair surfacing are given in Figure 5. The measurements of residual stresses, oriented along and across the specimen, were performed from the fusion line of a low-carbon sublayer with the base metal (determined by the macrostructure) deep into the metal. The values of residual stresses given on the plots are averaged over the thickness of the specimen.

The use of ultrasonic quartz sensors of longitudinal and shear waves with a base of measuring 7×7 mm did not allow making measurement of stresses closer than 1 mm to the fusion line of a low-carbon sublayer with the base metal. The maximum longitudinal residual tensile stresses σ_x are located directly in the area of repair surfacing and amount to about 240 MPa at a distance of 1 mm from the fusion line (Figure 5, *b*). At a distance of 40 mm from the place of repair surfacing, the residual longitudinal tensile stresses σ_x at a distance of 1 mm from the fusion line are in the range of 160–220 MPa (Figure 5, *a*, *c*). At a further distance from the fusion line deep into the metal, a zone of residual compressive stresses is formed, which reach the values of up to –70– –120 MPa in the cross-sections 1, 2 and up to –200 MPa in the cross-section 3 (in the area of repair surfacing). A significant volume of deposited metal during repair surfacing leads to the formation of higher transverse residual tensile stresses at 280 MPa in this area as compared to manufacturing surfacing (Figure 5).

After measurements of residual stresses, the specimens of the third series were tested for fatigue at a three-point zero-cycle bending. The cyclic life of the specimens before and after repair surfacing is given in Table 4.

After repair surfacing, initiation and propagation of fatigue cracks in all the specimens of the third series took place at a distance from the repair place. As in the case of manufacturing surfacing, the process of fatigue fracture of the parts restored by surfacing occurred either at the fusion boundary of individual beads, or directly near this boundary, apparently as a result of chemical and structural heterogeneity in this area (Figure 6, *a*).

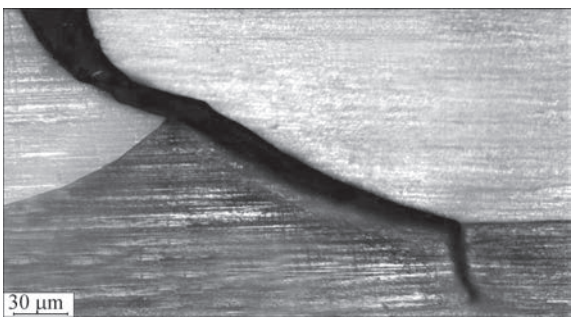

Figure 6. Appearance of the specimen area after repair surfacing with the formed fatigue crack, passing along the boundary between adjacent welded beads

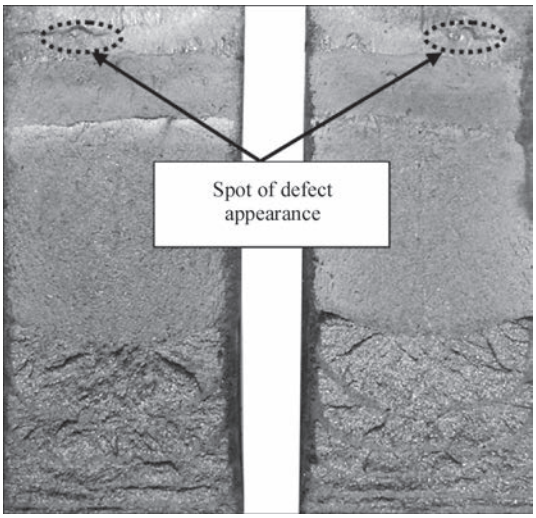

Figure 7. Appearance of fracture surface of the specimen No.10 with a defect along the fusion boundary between the individual layers of the deposited metal, from which fatigue crack was formed

Table 4. Results of fatigue tests of specimens of the third series

Number of specimen	Maximum cycle stresses, MPa	Cyclic life before formation of a crack of 10–12 mm, cycles	Cyclic life after repair surfacing, cycles	Total cyclic life, cycles
9	500	2127600	616300	2743900
10	600	461600	86900	1331100
11	600	2024700	109600	2134300

A low cyclic life of the specimen No.10 before the formation of a through crack with a length of 10–12 mm (Table 4) is predetermined by a technological defect of surfacing, which contributed to the early appearance of a crack inside the specimen (at a distance of 5 mm from the surface) in the fusion zone between individual layers of metal (Figure 7). Subsequently, at first the crack propagated in the wear-resistant metal before reaching the surface, and then in a low-carbon sublayer. After repair surfacing of the specimen No.10, initiation and propagation of a new fatigue crack occurred at 10–20 mm from the place of repair.

In general, it was confirmed that on the specimens No.9 and No.11 (Table 4), the application of repair surfacing to the products with fatigue cracks after their long-term operation does not lead to a significant increase in cyclic life after repair. This is associated with the fact that after long-term operation, the defect-free layer of deposited metal has a significant level of accumulated fatigue damages. Therefore, the repair of only a part of a product damaged by a fatigue crack without a complete removal of the deposited metal layer is inefficient.

However, considering the full cycle of a deposited part existence (manufacturing surfacing, operation, repair surfacing, operation), the proposed technology of repair surfacing using a ductile sublayer allowed increasing the total life of a deposited specimen by approximately 1.4 times as compared to the specimens deposited without a sublayer [7].

Nevertheless, based on the abovementioned data, in order to improve the efficiency of repair surfacing during repair of long-term operated products and to significantly increase the total life, it is recommended to remove not only the metal around the detected fatigue cracks, but the entire deposited layer to a depth of detected fatigue cracks with a subsequent restoration surfacing.

Conclusions

1. The technology of manufacturing and repair surfacing of specimens of carbon steel 40Kh, deposited using flux-cored wire PP-Np-25Kh5FMS with a sublayer of a low-carbon steel 08kp was developed. The non-destructive ultrasonic method for measuring stresses showed that the maximum longitudinal residual tensile stresses are located directly in the area of repair surfacing and amount to about 240 MPa at a distance of 1 mm from the fusion line of a low-carbon sublayer with the base metal. At a distance of 40 mm from the place of repair surfacing, the longitudinal residual tensile stresses at a distance of 1 mm from the fusion line are in the range of 160–220 MPa. A significant volume of deposited metal during repair surfacing leads to the formation of higher transverse residual tensile stresses at a level of 280 MPa in this area as compared to the manufacturing surfacing.

2. It was established that the main crack predominantly propagates along the fusion boundary of individual beads. In the process of fatigue fracture in the transition zones of a one metal layer to another, slight side branching from the main crack were observed, which propagated along the fusion line of the wear-resistant metal layer with the sublayer metal and along the fusion metal layer of the sublayer with the base metal. We suggest that such behavior is caused by the presence of a zone of chemical and structural heterogeneity in the areas of overlap of adjacent welded beads, which negatively affects the properties of materials and stress raisers predetermined by the geometry of adjacent deposited beads, which should be taken into account during development of technique and technology of repair surfacing.

3. The growth rate of fatigue cracks in different layers of metal of a multilayer material was experimentally investigated and the KDFF was constructed. It was established that the range of changes in the growth rate of fatigue cracks in the multilayer material corresponds to the linear area of KDFF, and accordingly can be described by the degree dependence of Paris $dl/dN = C(\Delta K)^m$ with the parameters $C = 5.75 \cdot 10^{-17}$ and $m = 4.87$. The maximum SIF values (140–180 MPa$\sqrt{m}$) obtained on the specimens with multilayer surfacing with a sublayer, is 2–3 times higher than the maximum SIF values obtained on the specimens without a sublayer, which indicates the rationality of a low-carbon sublayer to improve the crack resistance of multilayer material with a wear-resistant surfacing.

4. It was established that the cyclic life of the specimens of carbon steel 40Kh, deposited with the use of flux-cored wire PP-Np-25Kh5FMS with a sublayer of a low-carbon steel 08kp exceeds the cyclic life of the specimens deposited without a sublayer approximately by 2 times. Thus, the cyclic life of the specimens without a sublayer at maximum stress levels of 500 MPa is in the range of 561–1420 thou cycles of stress changes, and the cyclic life of the defect-free specimens with a sublayer at maximum stress levels of 500–600 MPa exceeds 2000 thou of cycles.

1. Du Toit, M., Van Niekerk, J. (2010) Improving the life of continuous casting rolls through submerged arc cladding with nitrogen-alloyed martensitic stainless steel. *Welding in the World*, 54(**11–12**), 342–349. DOI: https://doi.org/10.1007/bf03266748
2. Vundru, C., Paul, S., Singh ,R., Yan, W. (2018) Numerical analysis of multi-layered laser cladding for die repair applications to determine residual stresses and hardness. *Procedia Manufacturing*, 26, 952–961. DOI: https://doi.org/10.1016/j.promfg.2018.07.122
3. Gao, F., Zhou, J., Zhou, J. et al. (2017) Microstructure and properties of surfacing layers of dies manufactured by bimetal-gradient-layer surfacing technology before and after service. *The Int. J. Adv. Manuf. Technol.*, **88**, 1289–1297. DOI: https://doi.org/10.1007/s00170-016-8679-0
4. Zhang, J., Zhou, J., Tao, Y. et al. (2015) The microstructure and properties change of dies manufactured by bimetal-gradient-layer surfacing technology. *Ibid*, 80, 1807–1814 (2015). DOI: https://doi.org/10.1007/s00170-015-7170-7
5. Ahn, D.-G. (2013) Hardfacing technologies for improvement of wear characteristics of hot working tools: A Review. *Int. J. of Precision Engineering and Manufacturing*, 14 (**7**), 1271–1283. DOI: https://doi.org/10.1007/s12541-013-0174-z
6. Jhavar, S., Paul, C.P., Jain, N.K. (2013) Causes of failure and repairing options for dies and molds: A review. *Engineering Failure Analysis*, 34, 519–535. DOI: https://doi.org/10.1016/j.engfailanal.2013.09.006
7. Ryabtsev, I.O., Knysh, V.V., Babinets, A.A. et al. (2020) Fatigue life of specimens after wear-resistant, manufacturing and repair surfacing. *The Paton Welding J.*, **9**, 19–25. DOI: https://doi.org/10.37434/tpwj2020.09.03
8. Rjabcev, I.A., Senchenkov, I.K., Turyk, Je.V. (2015) *Surfacing. Materials, technologies, mathematical modeling*. Gliwice, Wydawnictwo politechniki slaskiej.
9. Korotkov V.A. (2017) More efficient surfacing. *Russian Engineering Research*, 37, 701–703. DOI: https://doi.org/10.3103/S1068798X17080093
10. Shao, C., Cui, H., Lu, F., Li, Z. (2019) Quantitative relationship between weld defect characteristic and fatigue crack initiation life for high-cycle fatigue property. *Int. J. of Fatigue*, 123, 238–247. DOI: https://doi.org/10.1016/j.ijfatigue.2019.02.028
11. Liu, H., Yang, S., Xie, C. et al. (2018) Mechanisms of fatigue crack initiation and propagation in 6005A CMT welded joint. *J. of Alloys and Compounds*, **741**, 188–196. DOI: https://doi.org/10.1016/j.jallcom.2017.12.374
12. Zerbst, U., Madia, M., Beier, H.T. (2017) Fatigue strength and life determination of weldments based on fracture mechanics. *Procedia Structural Integrity*, **7**, 407–414. DOI: https://doi.org/10.1016/j.prostr.2017.11.106
13. Ryabtsev, I.A., Knysh, V.V., Babinets, A.A. et al. (2019) Methods and specimens for comparative investigations of fatigue resistance of parts with multilayer surfacing. *The Paton Welding J.*, **2**, 29–34. DOI: https://doi.org/10.15407/tpwj2019.02.05
14. Oberg, E. et al. (1996) *Machinery's Handbook.* 25th Ed. Industrial Press Inc.
15. (2004) *Device for control of mechanical stresses and strains in solid media.* Pat. UA 71637 C2 [in Ukrainian].
16. Kaierle, S., Overmeyer, L., Alfred, I. et al. (2017) Single-crystal turbine blade tip repair by laser cladding and remelting. *CIRP J. of Manufacturing Sci. and Technology*, **19**, 196–199. DOI: https://doi.org/10.1016/j.cirpj.2017.04.001
17. Caccese, V., Blomquist, P. A., Berube et al. (2006) Effect of weld geometric profile on fatigue life of cruciform welds made by laser/GMAW processes. *Marine Structures*, 19(**1**), 1–22. DOI: https://doi.org/10.1016/j.marstruc.2006.07.002
18. Murakami, Yu. (1990) *Reference book on stress intensity coefficients.* In: 2 Vol. Moscow, Mir [in Russian].

Received 05.02.2021

INTERNATIONAL CONFERENCE
STATE-of-the-ART TECHNOLOGIES for JOINING MATERIALS
31 May – 2 June 2021
Kyiv, E.O. Paton Electric Welding Institute of the NAS of Ukraine

Topics of the Conference:
- arc welding and surfacing
- beam and plasma technologies of welding, surfacing and coating
- hybrid welding processes
- friction stir welding
- resistance butt welding
- 3D additive technologies based on welding processes

Organizing committee
Tel./Fax: (38044) 200-82-77
E-mail: journal@paton.kiev.ua
www.pwi-scientists.com/eng/modernweld2021